Ultrafast Generation of Ferromagnetic Order via a Laser-Induced Phase Transformation in FeRh Thin Films

Ganping Ju,[1,*] Julius Hohlfeld,[1] Bastiaan Bergman,[1,2] René J. M. van de Veerdonk,[1] Oleg N. Mryasov,[1] Jai-Young Kim,[1] Xiaowei Wu,[1] Dieter Weller,[1] and Bert Koopmans[2]

[1]*Seagate Research, 1251 Waterfront Place, Pittsburgh, Pennsylvania 15222, USA*

[2]*Department of Applied Physics, Eindhoven University of Technology, P.O. Box 513, 5600 MB, Eindhoven, The Netherlands*

(Received 9 March 2004; published 4 November 2004)

It is demonstrated that ultrafast generation of ferromagnetic order can be achieved by driving a material from an antiferromagnetic to a ferromagnetic state using femtosecond optical pulses. Experimental proof is provided for chemically ordered FeRh thin films. A subpicosecond onset of induced ferromagnetism is followed by a slower increase over a period of about 30 ps when FeRh is excited above a threshold fluence. Both experiment and theory provide evidence that the underlying phase transformation is accompanied, but not driven, by a lattice expansion. The mechanism for the observed ultrafast magnetic transformation is identified to be the strong ferromagnetic exchange mediated via Rh moments induced by Fe spin fluctuations.

DOI: 10.1103/PhysRevLett.93.197403 PACS numbers: 78.47.+p, 75.30.Kz, 75.40.Gb, 75.50.Bb

The dynamic response of magnetic order to ultrashort external excitations is one of the challenging issues of modern magnetism, with potential impact on both fundamental science and technological applications, such as spintronic devices and the fundamental speed limits of magnetic recording. Over the past years, novel approaches have explored the elementary interactions between spins, electrons, and lattice when these systems are far from equilibrium. This distinguishes ultrafast magnetization dynamics from a (quasi-)static response. To date, three key experimental approaches are being pursued to initiate ultrafast magnetization dynamics. Two of them use femtosecond (fs) laser pulses either to affect magnetic order via ultrafast heating [1–4] or to induce weak magnetization via spin-selective optical excitation [5,6]. The third uses short field pulses to initiate magnetization precession in ferromagnets [7–10] or to induce transient magnetization in nonmagnetic materials [11]. Here we present a novel route exploiting ultrafast generation of ferromagnetism, which, despite its tremendous potential for applications, has not been reported.

A well suited material for the study of such a dynamic buildup of ferromagnetic order is FeRh in the chemically ordered CsCl crystal structure. This compound undergoes a phase transformation from antiferromagnetic (AFM) to ferromagnetic (FM) order when heated above a transformation temperature $T_{\mathrm{tr}} \sim 370$ K [12,13]. At low temperatures, FeRh is AFM with local iron moments $\mathbf{m}_{\mathrm{Fe}} = \pm 3\mu_B$ and no appreciable moment on rhodium. At elevated temperatures, the system is FM with local iron and rhodium moments of $\mathbf{m}_{\mathrm{Fe}} \approx 3\mu_B$ and $\mathbf{m}_{\mathrm{Rh}} \approx 1\mu_B$, respectively [14]. The underlying microscopic mechanism for this transformation is still unclear. Kittel originally proposed a model based on lattice expansion driven exchange inversion [15]. Electronic heat capacity [16] and spin fluctuation [17] mechanisms have also been discussed. However, neither experimental nor theoretical studies have provided sufficient information to identify the microscopic origin of this transformation. Nothing is published about the speed of the transformation [18].

In this Letter, we present experimental evidence that ferromagnetic order can be induced on the picosecond (ps) time scale when femtosecond optical pulses are used to drive the AFM-FM transformation in FeRh films. An illustration of the magnetic transformation is shown in Fig. 1(a). Optical pump-probe experiments along with first-principles calculations reveal details about the physics involved in the transformation. The results indicate that the transformation occurs on a subps time scale *before* the lattice expands.

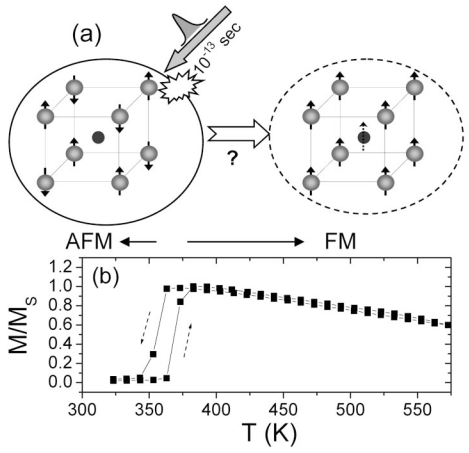

FIG. 1. (a) Schematic of the ultrafast generation of ferromagnetic order by inducing an AFM-FM transformation in FeRh when excited with femtosecond optical pulses. (b) Temperature dependence of the saturation magnetization of the annealed 100-nm-thick FeRh film.

The results presented in this Letter are obtained on a representative 100-nm-thick $Fe_{45}Rh_{55}$ film deposited via dc-magnetron sputtering onto a single crystalline MgO (100) substrate. The sample is heat treated by rapid thermal annealing at 975 K for 30 min to induce chemical ordering (CsCl structure). Specular x-ray diffraction technique scans (θ-2θ geometry) show strong (100) orientation and a high degree of chemical order [19]. As shown in Fig. 1(b), the temperature dependence of the magnetization, using a vector vibrating sample magnetometer with a magnetic field of 80 kA/m applied in the plane of the film, reveals the AFM-FM transformation at $T_{tr} \sim 360(350)$ K upon heating (cooling). Such temperature hysteresis is typical for FeRh thin film samples [13,19]. In the ferromagnetic phase, the magnetization lies in the film plane with negligible magnetocrystalline anisotropy.

The optical pump-probe experiments are performed using a Ti:sapphire pulsed-laser system with a pulse width of 100 fs and a repetition rate of 8 MHz. The fundamental beam ($\lambda = 800$ nm) is used for the optical excitation (pump) and is mechanically chopped at a frequency of 1.6 kHz. The second harmonic beam ($\lambda = 400$ nm) is used to measure the time-resolved pump-induced response (probe). The pump and probe beams are focused using a single objective lens [numerical aperture (NA) $\sim$0.7] to overlapping spots of about 6 and 3 μm diameters, respectively, at a 45° angle of incidence to the film normal. The magnetization dynamics is probed using the magneto-optical Kerr effect and is measured in a split beam configuration using a Wollaston prism followed by two photodetectors and lock-in amplification. A magnetic field of280 kA/m [20] is applied at a 45° angle to the sample normal in order to define the preferred magnetization direction and achieve high sensitivity to the polar Kerr signal [22]. The polarization (magnetization) change, $\Delta\theta_K(t)$, is detected as the difference voltage between the two detectors, while the sum detects the reflectivity change, $\Delta R(t)$. To avoid cross talk between polarization and reflectance signals, measurements at both positive and negative applied magnetic fields are conducted, where now the difference of $\Delta\theta_K(t)$ between the two field directions corresponds to only the transient magnetic response.

The transient Kerr effect traces as a function of pump-probe delay and excitation fluencies are shown in Fig. 2(a). Clearly, a threshold behavior is observed, with an onset of the pump-induced Kerr signal appearing for fluencies exceeding $F_{tr} \sim 5.3$ mJ/cm^2 in the present case. This is consistent with the interpretation that the pump-induced magnetization originates from the AFM-FM transformation. With further increase of the fluence a double peak feature is observed with one peak after about 20–35 ps, followed by a second peak after about 120 ps. This observation can be interpreted by assuming that the magnetization reaches a maximum when T_{tr} is reached and then decreases with further increase of temperature.

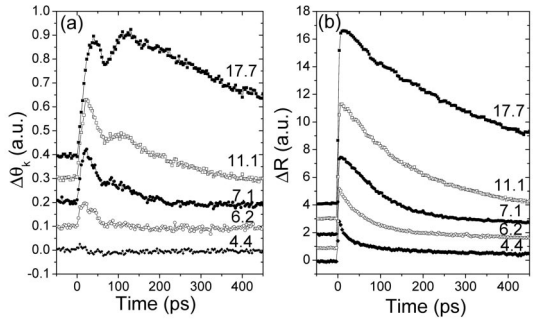

FIG. 2. Time evolution of (a) the transient Kerr effect $\Delta\theta_K(t)$ and (b) the transient reflectivity $\Delta R(t)$ as a function of pump fluences (labeled for each curve in mJ/cm^2). The curves are vertically displaced for clarity.

Upon cooldown, the magnetization traverses the magnetization peak again (see also remark [23]). Despite a focus ratio of two between the Gaussian pump and probe beams, nonuniform heating effects across the probed areas need to be considered to address the details of the fluence dependencies. The gradual increase of the two peaks in $\Delta\theta_K(t)$ is attributed to a larger portion of the probed area being excited above the transformation threshold with increasing fluence.

The transient reflectivity, on the other hand, shows a completely different behavior. As shown in Fig. 2(b), finite reflectivity changes are observed at all pump fluence levels. Below the transformation threshold, $\Delta R(t)$ reflects transient electron and lattice temperature dynamics [24]. In this regime, all curves fall on top of each other when normalized to the pump fluence. At fluence levels above the threshold, the signal amplitude increases and the dynamical response develops a different signature. This is better illustrated in Fig. 3(a), where two transient reflectivity traces measured with enhanced time resolu-

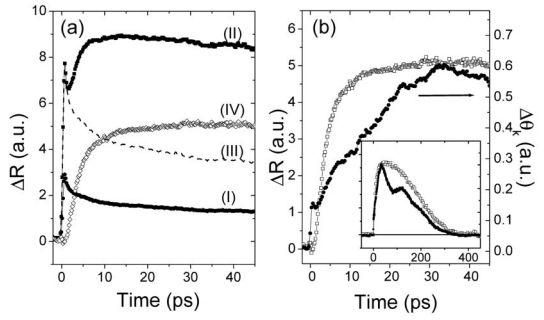

FIG. 3. (a) Transient reflectivity $\Delta R(t)$ at short times for subthreshold (I) and superthreshold fluence (II). The subthreshold $\Delta R(t)$ curve is normalized to the superthreshold curve [dashed line in (III)] and subtracted to reveal the nonelectronic lattice expansion contribution to $\Delta R(t)$ [open symbols in (IV)]. (b) Comparison of the dynamics of lattice expansion (open squares) and induced magnetization (solid circles), with the comparison at longer time scale shown in the inset.

tion for subthreshold and superthreshold fluence, respectively, are compared. The subthreshold curve shows a distinct jump at ~0.67 ps followed by a monotonic decrease [24,25]. By contrast, the superthreshold trace shows a second peak occurring at 5–10 ps. The coincidence of the fluence levels for the appearance of this second peak in $\Delta R(t)$ and $\Delta\theta_K(t)$ indicates that the AFM-FM transformation is accompanied by a lattice expansion. To separate the effect of lattice expansion [26] from the conventional electron/lattice thermalization and cooling process, a scaled subthreshold transient reflectivity curve is subtracted from the superthreshold fluence data, as illustrated in Fig. 3(a). The scaling factor is simply the fluence ratio [27]. The resulting curves indicate a rapid lattice expansion within the first 10 ps after an initial delay of about 1 ps, leveling off at ~20–40 ps.

A side-by-side comparison of the dynamics of the induced magnetization and lattice expansion is shown in Fig. 3(b). The magnetization shows a rapid initial rise within the first ps, which is on the same time scale as the hot electron thermalization response in the reflectivity. After this nucleation event, the magnetization grows at a significantly slower rate towards a maximum at about 30–35 ps, as discussed before. On longer time scales, as shown in the inset of Fig. 3(b), the induced magnetization vanishes at ~300 ps for pump fluence of 11.1 mJ/cm^2. The time required to cool below T_{tr} increases monotonically with excitation fluence. The extra contribution from the lattice expansion in the transient reflectivity disappears at the same time, further confirming that both the induced magnetization and lattice expansion originate from the AFM-FM transformation.

To clarify the underlying microscopic mechanism of the AFM-FM transformation in FeRh, first-principles calculations based on the constrained density functional theory within the local spin-density approximation (CLSDA) [28,29] are conducted. The CLSDA theory allows one to determine the electronic structure self-consistently for the general case of noncollinear magnetic order and enables the calculation of exchange interaction parameters [28,29] and analysis of atomic moment response to the thermal fluctuations [29,30]. An effective exchange parameter J^0, describing stability of magnetic order, can be defined as $J^0 = d^2E_{ex}/d^2\Theta$, where Θ is the angle defining the deviation of the Fe sublattice magnetization from the ground state orientation, and $E_{ex} = E_{Fe} + E_{Rh}$ is the total exchange interaction energy with contributions originating from Fe sublattice interactions and from induced Rh moments. Thus, two contributions to J^0 can be distinguished as a "direct" Fe-Fe exchange (J_{Fe}) and an "indirect" Rh-mediated exchange (J_{Rh}). The lattice spacing dependence of these exchange parameters is shown in Fig. 4(a). It is found that J_{Fe} remains negative, i.e., antiferromagnetic, within the range of lattice spacing of interest [21,31,32], whereas J_{Rh} is ferromagnetic and varies strongly with the value of the Rh spin moment. In addition, calculations of the lattice constant difference between the AFM and FM configurations yields $\delta a_{\text{AFM-FM}} = 0.015$ Å, in good agreement with experiment [21,31,32]. These findings support the experimental evidence, provided in Fig. 3, that the AFM-FM transformation in FeRh is accompanied, but not driven, by lattice expansion.

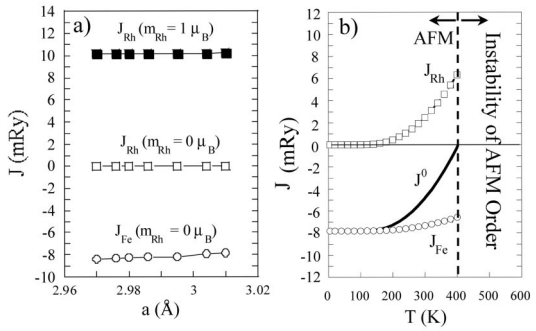

FIG. 4. (a) Lattice spacing (a) dependence of the competing AFM Fe-Fe exchange (J_{Fe}) and the effective Rh-moment mediated FM exchange (J_{Rh}), calculated for both $m_{Rh} = 0$ (AFM) and $m_{Rh} = 1\mu_B$ (FM). (b) Temperature dependence of the exchange parameters: J_{Fe}, J_{Rh}, and the sum $J^0 = J_{Fe} + J_{Rh}$. The vertical dashed line separates regions of stable and unstable AFM order.

In the following, we discuss how the spin subsystem itself can drive the transformation. Following earlier work on the origin of short-range order above T_C by Heine *et al.* [30], the dependence of the Fe and Rh spin moments on the constrained angle between the magnetization directions of the two sublattices is studied. The Fe atomic moment is found to be constant as a function of angle, indicating that it responds as a relatively localized moment to thermal fluctuations. On the other hand, the Rh atomic moment, $\mathbf{m}_{Rh}$, shows a nearly cosine behavior, indicating that Rh moment is induced by the exchange field of the Fe sublattice. It closely follows the relation $\mathbf{m}_{Rh} = \chi_{Rh}\mathbf{h}_{ex}$, where $\mathbf{h}_{ex}$ is the exchange field from the neighboring Fe sites and χ_{Rh} is an effective susceptibility. The energy change associated with the induced Rh moment, E_{Rh}, closely follows the Stoner model $E_{Rh} = -\tilde{I}\mathbf{m}_{Rh} \cdot \mathbf{m}_{Rh}$, which is used to calculate J_{Rh} contribution as shown in Fig. 4(a). This can be interpreted as an effective indirect ferromagnetic Fe-Fe exchange interaction, mediated by the induced Rh moment, as shown in Fig. 4(a). The Stoner model parameter is calculated to be as large as $\tilde{I} \sim 12$ mRy/f.u., which explains the strong Rh-mediated ferromagnetic exchange. As we illustrate with the following mean-field approximation calculations, this indirect exchange can become strong enough to create instability of AFM order above a certain level of fluctuations in the Fe sublattice.

The FeRh spin system can be considered as a mixture of localized Fe atomic moments, with interactions described within a Heisenberg model, and induced delocalized Rh moments, with interactions described by a Stoner

model, in contrast to the model in [17], where both Fe and Rh are treated as localized moments. As the Fe moments are thermally (or optically) excited, an increasing local random net exchange field exists on the Rh sites. The spin-temperature effect in the (overheated) AFM phase is illustrated using a mean-field calculation with $S = 3/2$ for the Fe sublattice. Figure 4(b) shows the calculated temperature dependence of the total effective exchange parameters (J^0), which is the sum of the exchange interaction contributions from both sublattices: J_{Fe} and J_{Rh}. In accordance with the Stoner model, the induced Rh moment (J_{Rh}) mediates ferromagnetic interaction of increasing strength as the temperature rises. Above a certain critical temperature where the amplitude of the Rh-moment fluctuations become sufficient such that the ferromagnetic interactions overcome the antiferromagnetic Fe-Fe exchange, magnetic order stability parameter J^0 crosses zero and FM nuclei can form.

Combining all results, the following interpretation of the experiments is proposed. Ferromagnetic order is first nucleated when the Fe sublattice of the antiferromagnetically ordered FeRh is excited above the AFM-FM transformation threshold. At this point, the spin fluctuations in the Fe sublattice result in a net local exchange field on the Rh sites. The indirect ferromagnetic exchange mediated by the induced Rh moment overcomes the direct antiferromagnetic Fe-Fe exchange interactions, tipping the overall balance in favor of ferromagnetic order. The local nucleation of ferromagnetism occurs on a similar subps time scale as the magnetization modulation observed in transition metal ferromagnets upon ultrafast photoexcitation [1–3]. A net exchange field will exist on the Rh sites at the boundary of the initially nucleated ferromagnetic domain, which will therefore expand. The equilibrium lattice constant of the ferromagnetically ordered state is larger than that of the AFM state. Therefore, the AFM-FM transformation is accompanied by a lattice expansion and stress relaxation as observed in the present experiments.

This work was performed as part of INSIC HAMR ATP Program, with the support of the U.S. Department of Commerce, National Institute of Standards and Technology, Advanced Technology Program, Cooperative Agreement No. 70NANB1H3056.

Note added in proof.—After the submission of the Letter, we became aware of a similar work by J. U. Thiele *et al.* [18] that was submitted on 7 May 2004.

*Electronic address: Ganping.Ju@Seagate.com

[1] E. Beaurepaire *et al.*, Phys. Rev. Lett. **76**, 4250 (1996).
[2] J. Hohlfeld *et al.*, Phys. Rev. Lett. **78**, 4861 (1997).
[3] G. Ju *et al.*, Phys. Rev. B **57**, R700 (1998).
[4] A. V. Kimel *et al.*, Phys. Rev. Lett. **89**, 287401 (2002).
[5] J. M. Kikkawa *et al.*, Nature (London) **397**, 139 (1999).
[6] A. V. Kimel *et al.*, Phys. Rev. B **63**, 235201 (2001).
[7] Th. Gerrits *et al.*, Nature (London) **418**, 509 (2002).
[8] H. W. Schumacher *et al.*, Phys. Rev. Lett. **90**, 017201 (2003).
[9] S. Kata *et al.*, Appl. Phys. Lett. **80**, 2958 (2002).
[10] C. H. Back *et al.*, Science **285**, 864 (1999).
[11] A. Y. Elezzabi *et al.*, Phys. Rev. Lett. **77**, 3220 (1996).
[12] M. Fallot *et al.*, Rev. Sci. **77**, 498 (1939).
[13] J. S. Kouvel *et al.*, J. Appl. Phys., Suppl. **33**, 1343 (1962).
[14] V. L. Moruzzi *et al.*, Phys. Rev. B **46**, 2864 (1992).
[15] C. Kittel, Phys. Rev. **120**, 335 (1960).
[16] P. Tu *et al.*, J. Appl. Phys. **40**, 1368 (1969).
[17] M. E. Gruner *et al.*, Phys. Rev. B **67**, 064415 (2003).
[18] J. U. Thiele *et al.*, Appl. Phys. Lett. **85**, 2857 (2004).
[19] J. U. Thiele *et al.*, Appl. Phys. Lett. **82**, 2859 (2003).
[20] We note that the in-plane applied field component needs to exceed ~120 kA/m in order to induce a single domain state in the sample. A further field increase has a similar effect as increasing the pump fluence above the AFM-FM threshold, consistent with the static measurement showing that the applied field reduces the transition temperature [21].
[21] J. B. McKinnon *et al.*, J. Phys. C **1**, S46 (1970).
[22] M. van Kampen *et al.*, Phys. Rev. Lett. **88**, 227201 (2002).
[23] We are aware of another mechanism that provides a double (or even multi) peaklike behavior in $\Delta\theta_K(t)$. In our configuration the initial growth of the magnetization will be accompanied by a strong increase of the demagnetization field. Such a rapid variation in the effective anisotropy field is known to give rise to precessional motion of the magnetization [20]. However, we carefully verified that including this effect does not affect our conclusions regarding the rapid transformation during the first tens of ps.
[24] Transient reflectivity has been widely used to study the electron-phonon relaxation dynamics. Three regimes can be typically recognized: (i) generation of nonequilibrium (hot) electrons; (ii) *e-e* scattering leads to thermalization at an elevated temperature T_e [observed as a hot electron peak in $\Delta R(t)$ around several hundred fs]; (iii) electron-phonon interactions equilibrate the electron and lattice systems (T_l) on a time scale of a few ps, followed by lattice expansion and cooling on a longer time scale.
[25] C. K. Sun *et al.*, Phys. Rev. B **50**, 15 337 (1994).
[26] We note that the AFM-FM transition induced ΔR contains both contributions from lattice expansion and electronic band-structure change. However, we observed a delay of 1 ps in the subtracted ΔR data without a subps jump (as observed in $\Delta\Theta_K$) that would be expected for the case with a significant electronic contribution. This leads to the conclusion that the dominant contribution to the AFM-FM phase-change induced ΔR is from the transition-driven lattice expansion.
[27] The subtraction based on linear scaling is further justified by the fact that the linear relation between the hot electron peak and the pump fluence is still maintained above the transformation threshold.
[28] O. N. Mryasov *et al.*, Phys. Rev. B **45**, 12 330 (1992).
[29] M. Uhl and J. Kubler, Phys. Rev. Lett. **77**, 334 (1996).
[30] V. Heine *et al.*, Europhys. Lett. **12**, 545 (1990).
[31] G. Shirane *et al.*, Phys. Rev. **131**, 183 (1963).
[32] M. R. Ibarra *et al.*, Phys. Rev. B **50**, 4196 (1994).